Biomaterials Advances 169 (2025) 214182

Contents lists available at ScienceDirect

Biomaterials Advances

journal homepage: www.journals.elsevier.com/materials-science-and-engineering-c

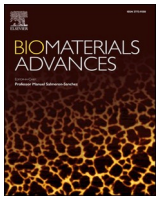

# A practical workflow for cytocompatibility assessment of living therapeutic materials

Joëlle Aurelie Mekontso [a,b], Usama Farrukh [a,b], Sara Trujillo [a,*], Aránzazu del Campo [a,b,*]

[a] INM-Leibniz Institute for New Materials, Saarbrucken, Germany
[b] Chemistry Department, Saarland University, 66123 Saarbrucken, Germany

ARTICLE INFO

*Keywords:*
Living therapeutic materials
Cytocompatibility
Workflow
Bacterial hydrogels
Pluronic

ABSTRACT

Living Therapeutic Materials (LTMs) are a promising alternative to polymeric drug carriers for long term release of biotherapeutics. LTMs contain living drug biofactories that produce the drug using energy sources from the body fluids. To clarify their application potential, it is fundamental to adapt biocompatibility and cytotoxicity assays applied from non-living biomaterials and therapeutics to evaluate how LTMs interact with host cells. Here, we have established a first step in this direction, by developing a practical workflow to parallelize in vitro assessment of minimal safety and cytocompatibility properties of bacterial LTMs. It allows systematic monitoring and quantification of the dynamic evolution of the bacterial population (growth, metabolic activity) in parallel to quantify the response of different mammalian cells to LTM supernatants with regards to cytotoxicity and release of pro-inflammatory cytokines over a period of 7 days using a maximum of 10 samples. The protocol was tested with a Pluronic-based thin film containing *ClearColi*. The results show no cytotoxic effects of *ClearColi* containing hydrogels in three mammalian cell lines, and no induction of pro-inflammatory cytokines under the tested conditions. This workflow represents a first step in establishing a roadmap for the safety assessment of LTMs, and investigation of biocompatibility potential of future living therapeutic devices.

## 1. Introduction

Engineered living materials (ELMs) integrate engineered living cells (typically bacteria, yeast or viruses) [1–8] into inert materials to fulfill specific functions. In the medical field, ELMs have been explored for biosensing [9,10] and drug delivery [11,12] (so-called Living Therapeutic Materials, LTMs) due to their capability to produce reporter molecules, enzymes or other therapeutic molecules in contact with the body in response to specific stimuli [13]. For example, living wearable devices have been reported to detect molecules like N-acyl homoserine lactone, isopropyl β-d-1-thiogalactopyranoside, rhamnose and anhydrotetracycline in a multiplexed way by engineering *E. coli* and encapsulating them in Pluronic-F127 diacrylate-based hydrogels [14]. Living ingestible devices capable of sensing gastrointestinal bleeding with high specificity and sensitivity in vivo have also been reported [15]. Agarose-based ELMs embedding optogenetically engineered *E. coli* produced and secreted proteins [16] or antimicrobial drugs in response to blue light irradiation [3].

The application of LTMs requires previous quantification of the biocompatibility of the living devices with the host [17] and presents specific challenges associated with their living character. The microorganisms in the LTM consume nutrients from their environment and grow over time. Their behavior changes with oxygen and nutrient concentration in their environment, and so does their secretome. Therefore, biocompatibility assessment of LTMs needs to consider the dynamic properties of the LTM itself over time in response to changing environmental conditions, and across a representative time scale for an intended application scenario. The long-term stability of the hydrogel system is also an important parameter, as it is necessary not only to prevent the microorganisms from escaping into the surrounding medium, but also to maintain them functional. To address all these aspects, biocompatibility assays need to be extended to evaluate the dynamic responses of the host cells and the LTM itself.

A frequent LTM design in reported works from our group [18,19] and others [14,20,21] relies on Pluronic based hydrogels as encapsulating material. Typically, mixtures of Pluronic-F127 (Plu) and Pluronic-F127 diacrylate (PluDA) at 14–30 wt% concentrations are used. These hydrogels allow the diffusion of nutrients and gases necessary for bacteria growth. With increasing fraction of PluDA, bacteria growth and escape can be hindered [18,22]. Controlled and confined organism

* Corresponding authors.
*E-mail addresses:* sara.trujillomunoz@leibniz-inm.de (S. Trujillo), aranzazu.delcampo@leibniz-inm.de (A. del Campo).

https://doi.org/10.1016/j.bioadv.2025.214182
Received 11 October 2024; Received in revised form 8 January 2025; Accepted 8 January 2025
Available online 10 January 2025

growth in the LTM during weeks has been achieved using Pluronic hydrogels in a bilayer or a core-shell format. These hydrogels have storage Modulus between 18 and 43 kPa as the PluDA fraction in the mixture increases from 0 and 100 % [22]. These hydrogels allow the diffusion of nutrients and gases necessary for bacteria growth. With increasing fraction of PluDA, bacteria growth and escape can be hindered [18,22]. Microorganisms like *E. coli* [18–20,23], *Bacillus subtilis* [21], and yeast [23] have been encapsulated in these hydrogels. Secretion of a collagen-binding protein and sensing of L-Lactate have been demonstrated.

There are only a few reports where LTMs are assessed in terms of host reactions. The immune response to Plu/PluDA bacterial hydrogels containing *ClearColi* was evaluated on day 3 by exposing them to peripheral blood mononuclear cells (PBMCs) from different donors. Results showed that the shielded bacteria in the bilayer reduced cell activation and lowered the percentage of apoptotic cells. Immune response varied among donors, highlighting the need for comprehensive characterization of the effects of these devices [19]. In a different example, *Lactococcus lactis* engineered to produce an angiogenic factor and entrapped in a heparin-Pluronic hydrogel [24] was tested. The viability, proliferation and mobilization of human umbilical vein endothelial cells (HUVECs) were strongly enhanced, whereas the expression of CD86 in lipopolysaccharide (LPS) and interferon-γ (IFNγ)-stimulated macrophages was downregulated in contact with the vascular LTM supernatant. Pluronic hydrogels containing encapsulated *Bacillus subtilis* were tested to treat skin fungal infections in vivo [25]. Treatment of mice with the bacterial hydrogel after intradermal injection of *C. albicans* pseudohyphae resulted in minimal subacute inflammation after 4 days and no inflammation after 10 days. *Lactobacillus reuteri* within gelatin-hyaluronic acid hydrogels were investigated to treat bacterial-infected wounds, showing the antibacterial activity of L. *reuteri* in vitro and in vivo [26]. The bacterial hydrogels were not cytotoxic to mouse fibroblast L929 cells in vitro. Less inflammation, as well as faster healing were observed at the wound site in *Staphylococcus aureus*-infected mice and treated with the hydrogel. These examples show good biocompatibility, and low inflammatory response in mice. However, they are performed at individual time scales and number of organisms, and do not consider the dynamic character of the LTMs.

In this work, we present a practical workflow and corresponding detailed assay protocols for in vitro cytocompatibility testing of living materials and we apply it to assess cytocompatibility of a bacterial Plu/PluDA hydrogel containing *ClearColi* on a 7 day timescale. Our workflow is designed to minimize the time and resources investment in a parallelized characterization of the LTM evolution and the response (cytotoxicity, pyrogenicity and pro-inflammatory effects) of three mammalian cell lines to LTMs at 5 different time points using a maximum of 10 samples for a particular LTM design. The simplicity of the workflow facilitates application at early stages of LTM development and early detection of potential risks and stoppers for the later application of the LTM.

## 2. Materials and methods

All reagents were acquired from Sigma unless stated otherwise. Dulbecco's Phosphate Buffer Saline (DPBS, Gibco), Dulbecco's Modified Eagle Medium (DMEM, Gibco), RPMI 1640 medium (Gibco), fetal bovine serum (FBS, PAN biotech), MEM Non-Essential Amino Acids Solution (NEAAs, Gibco), GlutaMAX supplement (Gibco), Penicillin/Streptomycin (P/S, Gibco), AlamarBlue Cell Viability Reagent (Invitrogen), CytoTox 96 Non-Radioactive Cytotoxicity Assay (Promega), Human IL-6 DuoSet ELISA Kit (R & D Systems), Mouse IL-6 DuoSet ELISA Kit (R & D Systems), 13 mm glass coverslips (VWR), 96-well angiogenesis plate (Ibidi) were purchased from the above mentioned companies.

### 2.1. Bacteria culture

The endotoxin free *ClearColi*(R) BL21(DE3) strain (BioCat) was used. Electroporation with the plasmid pUC19 resulted in Ampicillin resistance.

*ClearColi* was cultured in LB medium supplemented with 2 % NaCl and 50 μg/mL Ampicillin for 18 h at 37 °C and 250 rpm in a shaker. An optical density at 600 nm (OD) between 1 and 1.5 was obtained and used for the preparation of the bacterial constructs.

### 2.2. Preparation of bilayer thin films

Pluronic diacrylate (PluDA) was synthesized according to a reported protocol [27]. 23 % *w*/w stock solutions of Plu and PluDA, each containing 0.2 % Irgacure in MilliQ water, were prepared and used to prepare 23 % w/w stock solutions with 1:1 mixture of Plu/PluDA. Glass coverslips were immersed in a solution of 0.5 % 3 (Trimethoxysilyl) propyl acrylate in 95 % ethanol for 4 h, washed in 95 % *V*/V ethanol and air dried. Bacteria suspensions in Plu, PluDA or Plu/PluDA at different ODs (0, 0.05, 0.5, 0.8) were prepared by diluting the bacteria suspension with the stock polymer solutions to the corresponding OD. All solutions were prepared at 4 °C: at this temperature Plu and PluDA solutions are fluids.

Hydrogel bilayers were prepared on top of a glass substrate. The bilayers were composed of an inner layer of 23 % *w*/w Plu/PluDA hydrogel containing the bacteria and an outer layer of 23 % w/w PluDA hydrogel. Ten samples for each OD (0, 0.05, 0.5, 0.8) were prepared in parallel, giving a total of 40 samples and 4 conditions tested within a full experiment. The bilayer thin film with an initial OD of 0 was used as a control. A drop of 2 μL of the Plu/PluDA mixture at the desired OD was pipetted on top of glass coverslips placed on ice. Parallelly, a 30 μL droplet of the PluDA solution was pipetted on a 10 × 10 $cm^2$ piece of parafilm placed on a flat surface in the sterile hood and left to rest for 15 min. The glass coverslip was inverted and pressed gently with ethanol sterilised tweezers against the 30 μL PluDA drop. The piece of parafilm, on which the glass coverslips were inverted, was exposed to UV light (365 nm, 6 $mWcm^{-2}$) for 1 min. The glass coverslips were transferred to a 24-well plate and the wells were filled with medium and immediately used for the experiment.

Two different incubation conditions were used in order to determine the differences in bacteria growth over time depending on the incubation medium. In method 1, the samples were incubated in 500 μL RPMI 1640 medium supplemented with 10 % FBS. Supernatants were discarded and refreshed with 500 μL medium after 24 h. After 24 h of incubation, supernatants were collected, frozen, and 500 μL medium was refreshed. The samples were incubated for 4 days and supernatants were collected. These supernatants were used for cytotoxicity testing and for the investigation of inflammatory response. In method 2, the samples were incubated in 500 μL DPBS for 24 h. Afterwards, the supernatant was discarded and replaced with 500 μL RPMI 1460 supplemented with 10 % FBS for the six following days. These samples were used for brightfield imaging and quantification of bacteria growth. Method 1 was chosen for the final workflow.

### 2.3. Sample preparation for the workflow

Forty samples in total were used to perform the experiments listed in the workflow. For each of the four initial ODs (0, 0.05, 0.5, 0.8), 10 samples were prepared. 40 μL stock solutions of Plu and PluDA were prepared as described in Section 2.2 for each initial OD. All steps prior to the UV-crosslinking were performed as described in Section 2.2. After UV-crosslinking, the samples were transferred to 24-well plates and incubated in 500 μL RPMI 1640 medium supplemented with 10 % FBS. After 24 h of incubation, the medium was discarded and replaced with fresh medium. Supernatants were collected and frozen after 24 h of incubation and medium was refreshed. After 4 d of incubation,

supernatants were collected and frozen. These supernatants were used for cytotoxicity testing, investigating the release of pro-inflammatory cytokines and quantification of glucose. Brightfield images of the samples were taken, and bacteria growth was quantified at 5 different time points (0 h, 24 h, 48 h, 72 h, and 7 d). Live/dead imaging was done after 3 d of incubation.

### 2.4. Diffusion properties of the bilayer thin films

Cytochrome C (MW ≈ 12.3 kDa, 20 mg/mL), chymotrypsinogen A (MW ≈ 25 kDa, 20 mg/mL), albumin (MW ≈ 67 kDa, 20 mg/mL), phosphorylase b (MW ≈ 97.2 kDa, 20 mg/mL) and lactate dehydrogenase (MW ≈ 140 kDa, 20 mg/mL) were encapsulated in the bilayer thin films. To achieve this, 5 μL of Plu (23 % *w*/w) were mixed with 5 μL PluDA (23 % w/w) and 10 μL of protein. Then, 2 μL from this mixture were pipetted on top of a glass coverslip placed on ice. The next steps were performed according to the protocol described previously (Section 2.2). For each protein, 3 samples were prepared, plus control hydrogels without bacteria or protein (3 samples, OD = 0). After transferring the constructs to a 24-well plate, two incubation conditions were investigated. First, 900 μL DPBS were added to each well. After 6 h, 24 h, 48 h and 5 d of incubation, 150 μL supernatant were transferred to a microcentrifuge tube. As for the second alternative, 500 μL DPBS were added to each well and supernatant collection was performed only after 5 d of incubation. The supernatants were then used to conduct the Bicinchoninic Acid Assay (BCA) assay (Micro BCA Protein Assay Kit, Thermo Scientific) following manufacturer's instructions.

Briefly, standard curves for the BCA assay were prepared with known concentrations of all proteins ranging from 0.5 μg/mL to 200 μg/mL. The Micro BCA working reagent was prepared by combining 4 mL of Reagent MA and 3.84 mL Reagent MB with 0.16 mL of Reagent MC. Then, 150 μL of each standard or unknown sample replicate were pipetted into a microplate well. 150 μL of the WR were equally pipetted to each well and the plate was thoroughly shaken for 30 s. Afterwards, the plate was covered using a sealing tape and incubated at 37 °C for 2 h. The plate was then cooled to room temperature and absorbance was measured at 562 nm with a Tecan Spark® plate reader.

The Plasmid PSIP mCherry (6448 bp, 4000 kDa, 297 ng/μL) was encapsulated in the bilayer thin films. The plasmid map is shown in Fig. S1. For this purpose, 6.5 μL of Plu (23 % *w*/w) were mixed with 6.5 μL PluDA (23 % w/w) and 7 μL of plasmid. Then, 2 μL from this mixture were pipetted on top of a glass coverslip placed on ice. The next steps were performed according to the protocol described previously (Section 2.2). Three samples containing the plasmid were prepared, plus control hydrogels without bacteria or plasmid (3 samples, OD = 0). After transferring the constructs to a 24-well plate, 500 μL RPMI 1640 supplemented with 10 % FBS were added to each well and the samples were incubated at 37 °C. After 24 h, 48 h, 72 h and 7 d of incubation, 50 μL supernatant were collected and frozen. The supernatants were then used to conduct DNA quantification (Invitrogen™ Quant-iT™ PicoGreen™ dsDNA Assay-Kit) following manufacturer's instructions. 2 μg/mL stock solution of dsDNA were prepared by mixing 3 μL of the DNA standard with 147 μL of TE. A low-range standard curve from 250 pg/mL to 25 ng/mL was prepared starting from a 50 ng/mL DNA stock solution. 100 μL of the aqueous working solution of the Quant-iT™ PicoGreen™ dsDNA Reagent were added to each well. After mixing properly and incubating for 5 min at room temperature and protected from light, fluorescence was measured at 480/520 nm with a Tecan Spark® plate reader. 50 μL supernatants were mixed with 50 μL TE and added to a 96-well plate. 100 μL of the aqueous working solution of the Quant-iT™ PicoGreen™ dsDNA Reagent were added to each sample. Fluorescence was measured using the same instrument parameters as previously described. The fluorescence value of the reagent blank was subtracted from that of each of the samples and DNA concentration was determined using the generated standard curve.

### 2.5. Brightfield imaging of the bilayer thin films

Brightfield images of the samples containing *ClearColi* and incubated in RPMI 1640 supplemented with 10 % FBS were taken every 24 h throughout the duration of the experiments (7 days) using the Nikon Eclipse TI-E microscope equipped with an Andor Clara 16-bit CCD camera (1392 × 1040 pixels) at a 4× magnification. This experiment was conducted with samples prepared with both methods 1 and 2 (Section 2.2).

### 2.6. Live/dead staining of thin films and imaging

For the live/dead staining of samples prepared using method 1 (Section 2.2) after 3 d of incubation, first the RPMI medium was discarded, and the samples were washed with 1 mL DPBS to remove traces of the medium. Equal volumes of SYTO 9 dye (3.34 mM) and Propidium iodide (20 mM) were mixed. 3 μL from this dye mixture were added to 1 mL DPBS. Then, 100 μL of the staining solution were pipetted on top of the bacterial hydrogels and incubated for 30 min protected from light. The samples were washed with 1 mL DPBS once and fluorescence imaging was performed using the Leica DMI6000 B microscope at a 10× magnification.

### 2.7. Glucose quantification in bacterial supernatants

Glucose was quantified in the supernatants derived from the incubation of bilayer thin films in RPMI 1640 medium. These supernatants were collected from samples prepared with method 1 (Section 2.3) after 24 h and 5 d of incubation. The bilayer thin films without bacteria (OD = 0) were used as controls. The quantification of glucose from bacterial supernatants was performed with the glucose colorimetric detection kit (Invitrogen) following leaflet instructions. Briefly, a Glucose standard was prepared by serial dilution (32 mg/dL to 0 mg/dL). The supernatants were diluted 1:5 or 1:10 with Assay Buffer given the high concentration of glucose in RPMI medium (2000 mg/L). 30 μL Horseradish Peroxidase Concentrate (HRP, 100×) were mixed with 2.97 mL Assay Buffer to obtain 3 mL 1× HRP solution. 275 μL Glucose Oxidase Concentrate (10×) were mixed with 2.475 mL Assay Buffer to obtain 2.75 mL 1× Glucose Oxidase.

20 μL of glucose standards or of supernatants diluted 1:5 or 1:10 with assay buffer, followed by 25 μL 1× HRP solution were added to the wells. 25 μL Substrate and 25 μL 1× Glucose Oxidase were added to the wells. After incubating for 30 min at room temperature, absorbance was read at 560 nm with a Tecan Spark® plate reader.

### 2.8. Mammalian cell culture

Murine fibroblasts (NIH-3 T3 cells, ATCC, passages 5–23) were cultured in DMEM supplemented with 1 % P/S and 10 % FBS. Cell culture medium was exchanged every other day. Cells were split when 70 % confluency was reached (trypsin-EDTA, 3 min at 37 °C, 5%CO2).

Human monocytes (MONO-MAC 6 cells, ATCC, passages 2–9) were cultured in RPMI 1640 medium supplemented with 1 % P/S, 1 % Oxaloacetate, Pyruvate, and Insulin (OPI), 1 % Glutamax, 1 % NEAAs and 10 % heat inactivated FBS. Cell culture medium was exchanged every other day and cells were diluted to 300,000 cells/mL every 3–4 days (counted as passage).

Murine macrophages (J774A.1 cells, ATCC, passages 2–9) were cultured in DMEM supplemented with 1 % P/S, 1 % Glutamax and 10 % FBS. Cell culture medium was exchanged every other day. When approximately 75 % confluence was reached, cells were passaged by dislodging them from the surface of the culture flask using a cell scraper.

### 2.9. Cytotoxicity testing of bacterial supernatants

Cells (J774A.1, NIH-3 T3 and MONO-MAC 6) were used for

cytotoxicity testing. 1250 cells per well were seeded in an ibidi μ-Plate 96-well and cultured for 3 d. Afterwards, they were treated with 50 μL of bacterial supernatant from the bilayer films for 24 h. Conditions were analyzed in triplicates.

Lactate dehydrogenase assay (LDH) was used as per manufacturer's instructions to determine the percentage of cell death. First, positive controls were obtained by lysing the cells with Triton-X100 (5 μL of 37.5 % Triton-X 100) and mixing thoroughly. After 2 h, cells were considered completely lysed. Simultaneously, 5 μL DPBS were pipetted into the other wells to equilibrate the volumes. Afterwards, 30 μL of the culture supernatants were transferred to transparent bottom 96-well plates and 30 μL of LDH reagent were added on top and incubated for 30 min protected from light on an orbital shaker. After this incubation period, 30 μL stop solution were added to the wells to stop the reaction. Then, absorbance was measured at 490 nm ($A_{490}$) using a Tecan Spark® plate reader. Cells treated with culture medium were used as negative control.

To calculate the percentage of cell death for each time point, the following equation was used:

$$\text{Percentage of cell death} = \frac{A_{490}\ \text{treated cells}}{A_{490}\ \text{lysed cells}} \times 100 \quad (1)$$

AlamarBlue assay was performed to determine the number of cells metabolically active. After transferring the supernatants for the LDH assay to another well plate, 70 μL of 10 % AlamarBlue reagent in RPMI 1640 medium supplemented with 10 % FBS was used as per manufacturer's instructions. Then, the cells were incubated for 2 h, after which 60 μL supernatant were transferred to a dark bottom 96-well plate and fluorescence was measured at Ex/Em 570/600 nm with a Tecan Spark® plate reader.

Supernatants obtained from the samples prepared using method 1 (Section 2.3) were used to perform cytotoxicity testing. These supernatants were collected and frozen after 24 h and 5 d of incubation in RPMI 1640 medium supplemented with 10 % FBS. The positive control here were cells treated with culture medium.

### 2.10. AlamarBlue assay for quantification of bacteria proliferation in bilayer thin films

The AlamarBlue assay was also conducted to quantify bacteria in the bilayer thin films. Thin films were prepared with different initial bacteria ODs (0, 0.05, 0.5 and 0.8) and incubated in 500 μL RPMI 1640 medium supplemented with 10 % FBS. Every 24 h of incubation for 7 d, the medium was discarded and replaced with 500 μL 10 % AlamarBlue medium. The constructs were then incubated for 4 h, after which 100 μL supernatant were transferred to a dark bottom plate and fluorescence was measured as previously described. The AlamarBlue medium was then replaced with 500 μL RPMI 1640 medium and the constructs were incubated overnight. The samples with an initial OD of 0 were used as control.

### 2.11. Monocyte activation test to assess pyrogenicity of bacterial supernatants

10,000 MONO-MAC 6 cells in 10 μL growth medium were seeded per well in an ibidi μ-Plate 96-well. The cells were treated with 60 μL supernatant, growth medium (negative control) or LPS (positive control, 15 ng/mL). Cells were incubated for 24 h (37 °C, 5 % CO2) and then supernatants were collected and stored at −20 °C for the quantification of IL-6 secreted via ELISA.

### 2.12. Inflammation test with macrophages

The release of IL-6 from J774A.1 cells after treatment with supernatants was investigated. 10,000 J774A.1 cells in 50 μL growth medium were seeded per well in an ibidi μ-Plate 96-well and incubated for 24 h at 37 °C. After discarding medium from the wells, the cells were treated with 70 μL supernatant, growth medium (negative control) or LPS (positive control, 15 and 3.75 ng/mL). Cells were incubated for 24 h (37 °C, 5 % CO2) and then supernatants were collected and stored at −20 °C for the quantification of IL-6 secreted via ELISA.

### 2.13. Enzyme-linked immunosorbent assay (ELISA) for the quantification of IL-6

The protocols used to conduct these experiments were derived from the product datasheets of the Mouse (J774A.1 cells) and Human (MONO-MAC-6) IL-6 DuoSet ELISA Kits from R&D SYSTEMS. The reagents, standard dilutions, and samples were prepared as directed in the product. A 96-well microplate (Nunc MaxiSorp™) was coated with 100 μL of Capture Antibody per well. The plate was sealed and incubated overnight at room temperature. The following day, the plate was washed thrice by filling each well with Wash Buffer. The next step was blocking with 300 μL of Reagent Diluent per well. The plate was incubated for 1 h at room temperature and washed with wash buffer three times. Then, 100 μL of sample or standards in Reagent Diluent were added to each well (dilution 1:2.5) and incubated for 2 h at room temperature. The wash step was repeated. Then, 100 μL of the Detection Antibody were added to each well (2 h, room temperature). After incubation, samples were washed three times with wash buffer and 100 μL of Streptavidin-HRP were added to each well for 20 min (room temperature). The plate was washed again and 100 μL of Substrate Solution were added to each well (20 min, protected from light, room temperature). Lastly, 50 μL of Stop Solution were added to each well. The absorbance of each well was determined using a microplate reader set to 450 nm with a wavelength correction of 540 nm.

### 2.14. Statistical analysis

All experiments were performed with 6 replicates unless otherwise noticed. Statistical analysis was carried out using GraphPad Prism v9 software. All graphs represent the mean ± standard deviation (SD) unless otherwise noted. The goodness of fit of the data sets was assessed by Normality Shapiro-Wilk test. For comparisons of three groups, normal distributed populations were analyzed via analysis of variance (ANOVA) test followed by a Tukey's post hoc test to correct for multiple comparisons. For comparisons of two groups at different timepoints, populations were analyzed via analysis of variance (two-way ANOVA). Two-way ANOVA was performed by matching timepoint as a factor. A full model was fitted (time (row) effect, condition (column) effect and time/condition (row/column) effect). An equal variability of differences was not assumed and therefore the Geisser-Greenhouse correction was used. Multiple comparisons were performed two ways, first within each condition through time and then comparing conditions per timepoint (column (condition) and row (time) effects). Differences among groups are indicated as follows: $p$-values $<0.05$ (*), $p$-values $<0.01$ (**), $p$-values $<0.005$ (***), $p$-values $<0.001$ (****), and differences among groups not statistically significant (ns).

## 3. Results

As model LTM, bilayer Plu/PluDA hydrogel thin films containing *ClearColi* in the inner layer were prepared on glass substrates (Fig. 1) [18]. This format is appropriate for parallel preparation of different samples and culture in different external conditions. We used 23 % *w*/w PluDA hydrogel, which does not allow proliferation of bacteria, for the outer layer of the hydrogel, and a 1:1 Plu/PluDA mixture for the inner layer with the bacteria, which supports bacteria growth [18] (Fig. 1a). The bilayer hydrogels were prepared manually starting from stock solutions of the polymer at 4 °C. The hydrogels were further stabilized in the bilayer form by photocrosslinking. The bilayer hydrogels were transparent and allowed imaging of the growing colonies. The inner layer had a diameter of 2–3 mm, whereas the outer layer had a diameter

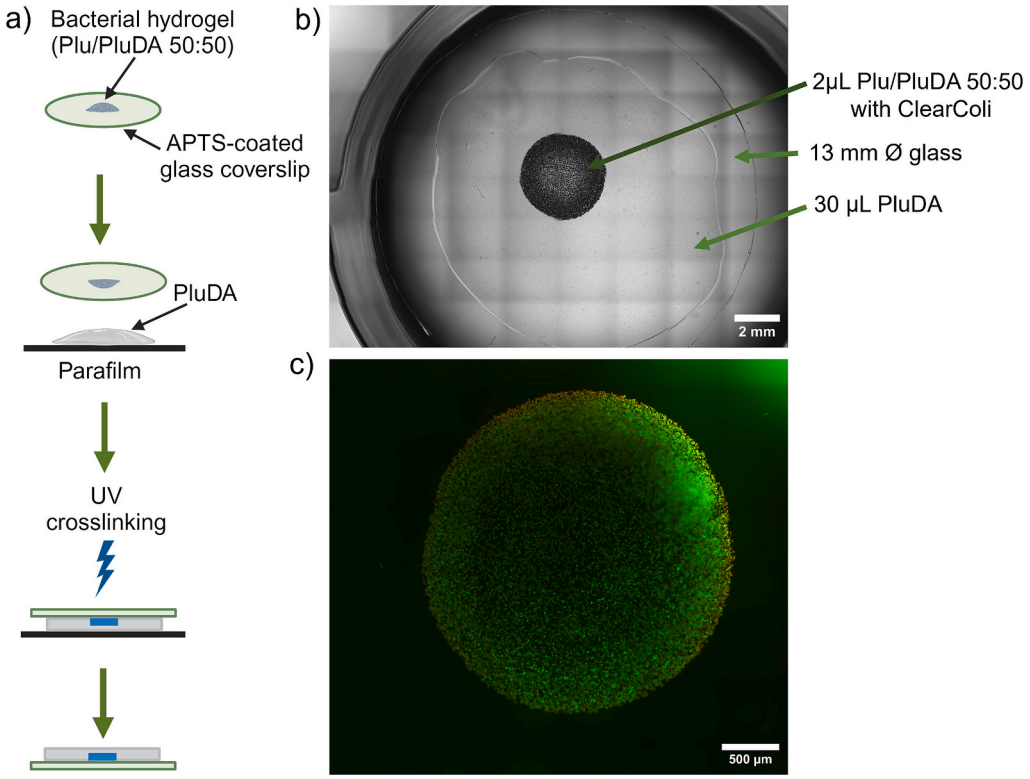


**Fig. 1.** Fabrication of the bilayer thin films.
(a) Fabrication steps to obtain the bilayer thin films. A droplet of Plu/PluDA bacterial solution is added to an APTS-coated glass coverslip. The coverslip is flipped and pressed on a larger droplet of PluDA on parafilm. Then, hydrogels are UV-crosslinked. (b) Macroscopic image of a bilayer thin film containing ClearColi (OD 0.5) on day 7 (scale bar: 2 mm). (c) Live/dead (green/red) image of a bilayer thin film containing ClearColi (OD 0.8) on day 1(scale bar: 500 μm). (For interpretation of the references to colour in this figure legend, the reader is referred to the web version of this article.)

of 10–11 mm. The thickness of the outer layer after swelling was about 100–150 μm (Fig. 1b). Bacteria were viable in the bilayer thin film after 24 h of incubation in RPMI 160 medium supplemented with 10 % FBS (Fig. 1c).

The diffusion properties of the encapsulating hydrogel determine how fast, and to what extent the host cells are exposed to the secretome of the LTM. This information is relevant for the selection of the timescale at which biocompatibility should be measured. We characterized the diffusion of large molecules through the bilayer thin films by adding proteins with molecular weight between 12.3 and 140 kDa to the inner layer solution before film formation. The release of the proteins to the supernatant was analyzed by the BCA assay of supernatants collected after 6 h, 24 h, 48 h and 5 d of incubation in DPBS (Fig. 2a). The smallest protein (cytochrome C) was released to the supernatant largely after 1 d and in full within 5 d. Larger proteins were released only partially within 5 days. We also studied diffusion for 5 d without exchanging medium (Fig. S2). Results show a similar trend, where the diffusion is dependent on molecular weight. We studied the diffusion of plasmids with a molecular weight of 4000 kDa (6448 bp) in a similar manner. A burst release of about 6 % of the initial amount encapsulated was observed during the first 24 h, and no further release at longer times (Fig. 2b). These results suggest that the Plu/PluDA bilayers allow slow release of large molecules, and studies at long time scales are necessary to detect larger molecules of the secretome in the supernatant.

LTMs are designed to contain the living organisms long term and prevent direct contact between organisms and host cells. Hence, host response is expected to be different than when the living therapeutic is directly applied to the body, without the shielding material. Therefore, biocompatibility testing of LTMs requires assuring that there is no leakage of organisms from the LTM during the tests. We investigated the leakage of bacteria from the bilayer films by determining the number of intact and contaminated samples after 1 d and 7 d of incubation (Fig. 2c). 85–90 % of the samples were not contaminated after 7 d. Contaminated samples leaked bacteria already after 24 h of incubation and this typically occurred at the interface between the bilayer and the glass substrate. Samples that contained higher initial OD (0.8) leaked more often and earlier (Fig. 2c). Samples that leaked during the study were discharged and not considered for further analysis.

Preliminary experiments were performed to investigate bacteria growth in the bilayer hydrogel at different conditions: i) variable initial bacteria density in the inner layer (OD = 0, 0.05, 0.5 and 0.8, which correspond to approximately 0, $10^5$, $10^6$ and $1.6{\cdot}10^6$ bacteria per sample), ii) growth time between 0 h and 7 d, iii) the growth medium with (RPMI 1640) and without nutrients (DPBS). *ClearColi* grew inside the inner layer in the form of discrete, rounded colonies, as observed in the brightfield microscopy images (Fig. 3). A faster colony growth was observed in the first 24 h of incubation, followed by a slower growth until 48 h and no further growth in the following 5 days of incubation. These morphological results are in agreement with previously reported works with bacterial Plu/PluDA hydrogels [18,19]. A higher number of colonies and a lower colony size was observed in the samples with higher initial OD, indicating that the growing neighbouring colonies consume the nutrients locally and restrict colony growth rate. Bacteria remained viable in the bilayer thin films for up to 7 days (Fig. S3).

We then quantified the growth in the bilayer thin films as function of nutrient availability. Different incubation conditions were tested: (i) direct incubation in RPMI 1640 medium and (ii) incubation in DPBS buffer solution for 24 h and medium exchange with RPMI 1640. Samples incubated in RPMI 1640 medium without medium exchange showed bacteria growth up to day 2 and no appreciable growth for longer culture times (Fig. 4a). Samples incubated in DPBS showed no growth within the first 24 h. Once DPBS was exchanged to RPMI 1640 medium,

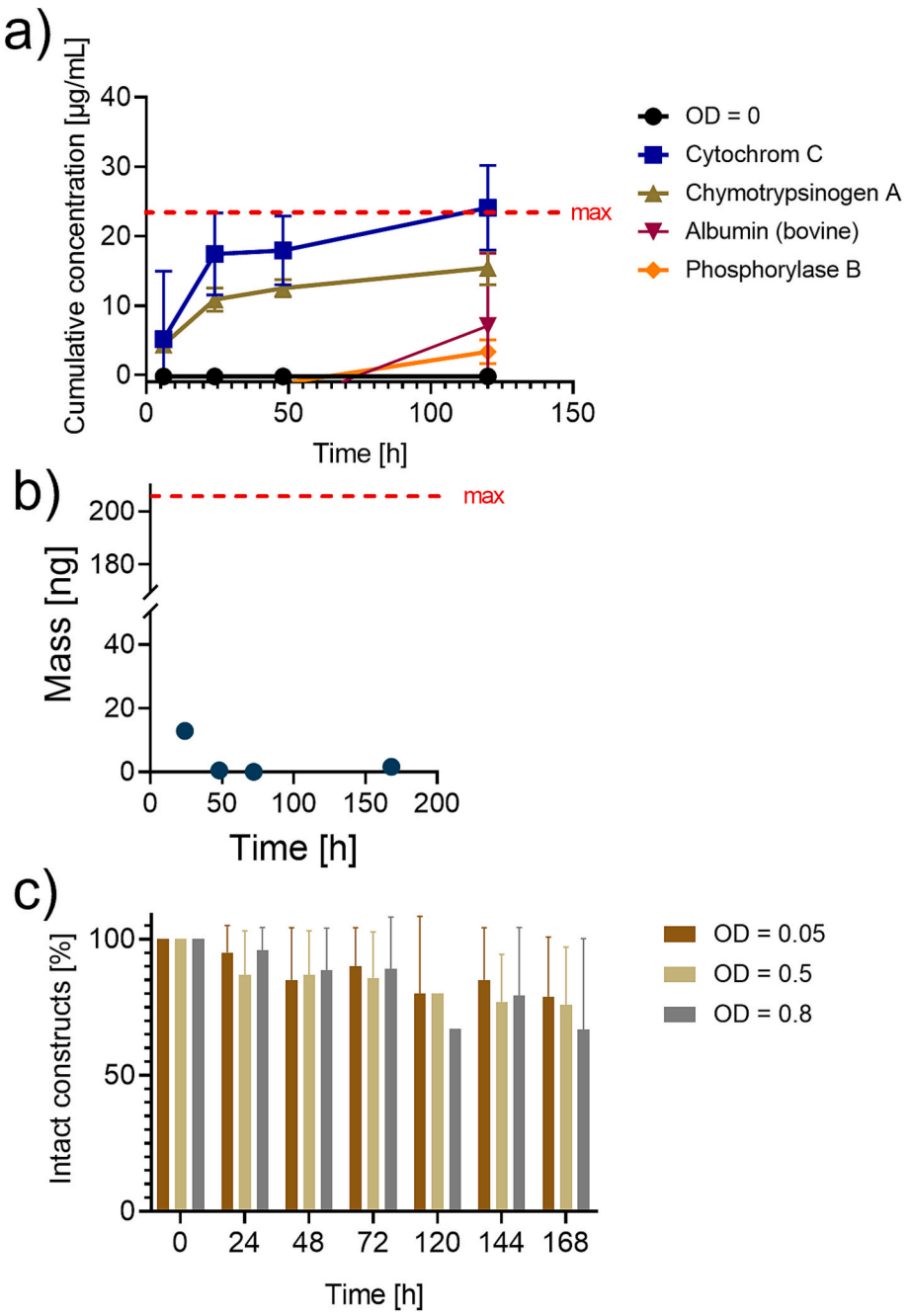


**Fig. 2.** Diffusion properties of the bilayer films.
(a) Release of cytochrome C (12.3 kDa), chymotrypsinogen A (25 kDa), albumin (67 kDa) and phosphorylase B (97.2 kDa) encapsulated in the bilayer thin films to the supernatant at times between 0 h and 5 d of incubation. Empty hydrogels without protein (OD 0) were used as controls. The concentration is represented in cumulative form (µg/mL, mean ± SD, $n = 3$). (b) Plasmid diffusion from bilayer thin films (plasmid PSIP mCherry, 6448 bp, 4000 kDa) between 0 h and 7 d (ng, mean ± SD, n = 3). Maximum release (marked in red) expected: 208 ng. (c) Percentage of intact constructs after 7 d of continuous incubation in RPMI 1640 medium supplemented with 10 % FBS. $n \geq 5$ constructs from four independent experiments. (For interpretation of the references to colour in this figure legend, the reader is referred to the web version of this article.)

bacterial growth was observed similarly as in the other conditions. In view of these results, we decided to incubate the bilayer thin films in RPMI 1640 medium immediately after fabrication to keep a constant nutrient supply.

The quantification of bacterial growth was performed by AlamarBlue assay. This assay quantifies proliferation as function of the metabolic activity of the cells. When grown in medium with nutrients, an increase in metabolic activity was observed during the first 48 h was seen, followed by a slower increase until 72 h. These results are in agreement with the microscopy observations. A decrease in the metabolic activity was observed at 7 d, probably due to the consumption of nutrients (Fig. 4b). The absence of nutrients during the first 24 h (experiment in DPBS) delayed the growth of bacteria and reduced the final at all incubation times (Fig. 4c).

Since we established that nutrient availability was necessary for the proliferation of bacteria during the first days of incubation, the direct incubation in RPMI 1640 medium was chosen for further experiments. This condition is also favourable to mammalian cells, which are fed with supernatants from these samples as they equally require nutrients for proliferation.

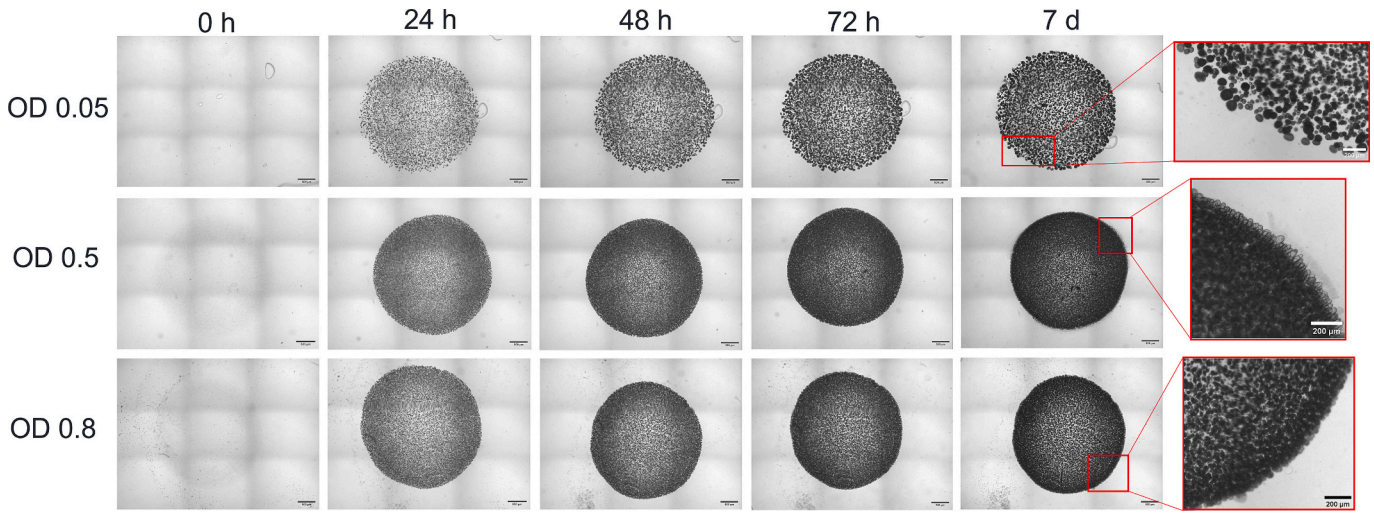


**Fig. 3.** Bacterial colonies inside bilayer thin films tracked by microscopy.
The images show the whole mount of the bilayer thin films at days 0, 1, 2, 3 and 7. Medium change was performed on days 1, 2, and 3. The images were taken at 4× magnification and stitched together. Samples were incubated in RPMI 1640 supplemented with 10 % FBS (scale bar: 500 µm). Highlighted in red are images at the interface between the inner and the outer layer (scale bar: 200 µm). (For interpretation of the references to colour in this figure legend, the reader is referred to the web version of this article.)

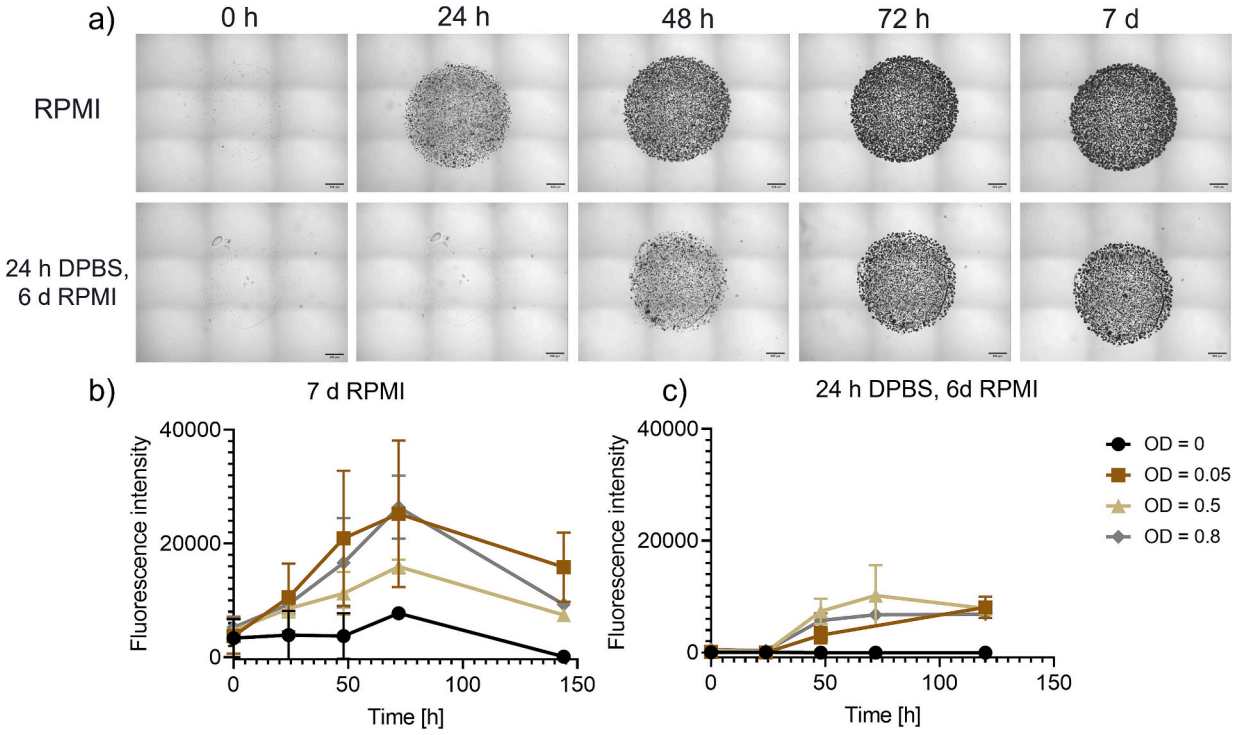


**Fig. 4.** Bacterial growth in different incubation media within the bilayer thin films.
(a) Whole mount images of thin films (OD 0.05) incubated in two different conditions (RPMI) 1640 medium supplemented with 10 % FBS continuously for 7 d (top row), and DPBS for the first 24 h, then medium change to RPMI 1640 supplemented with 10 % FBS for the following 6 d (bottom row). (b) Fluorescence intensity (arbitrary units) measured from AlamarBlue assay in the bilayer thin films incubated in RPMI 1640 + 10 % FBS during 7 d. (c) Fluorescence intensities measured from AlamarBlue assay in the bilayer thin films incubated in DPBS for the first 24 h and then medium exchange to RPMI 1640 + 10 % FBS for 6 d (mean ± SD, $n = 3$). Empty hydrogels (OD 0) were used as controls.

Once the conditions for bacteria growth had been investigated, we proceeded with the design of the workflow to assess the cytocompatibility of our model living material with different cell types. The workflow should maximize the output in terms of in vitro cytocompatibility data of an LTM with the minimum number of samples needed for statistical significance and minimize invested time. It minimizes the number of assays that require sample destruction and relies on complementary assays performed with the supernatant of a single sample.

Fig. 5 represents the resulting practical workflow. It assesses bacterial proliferation, viability and leakage of the bilayer and the cytotoxicity, pyrogenicity and pro-inflammatory effects of the supernatant over the span of 7 d starting from a set of 10 samples including 3 technical repetitions. It includes the following assays: (i) brightfield imaging and

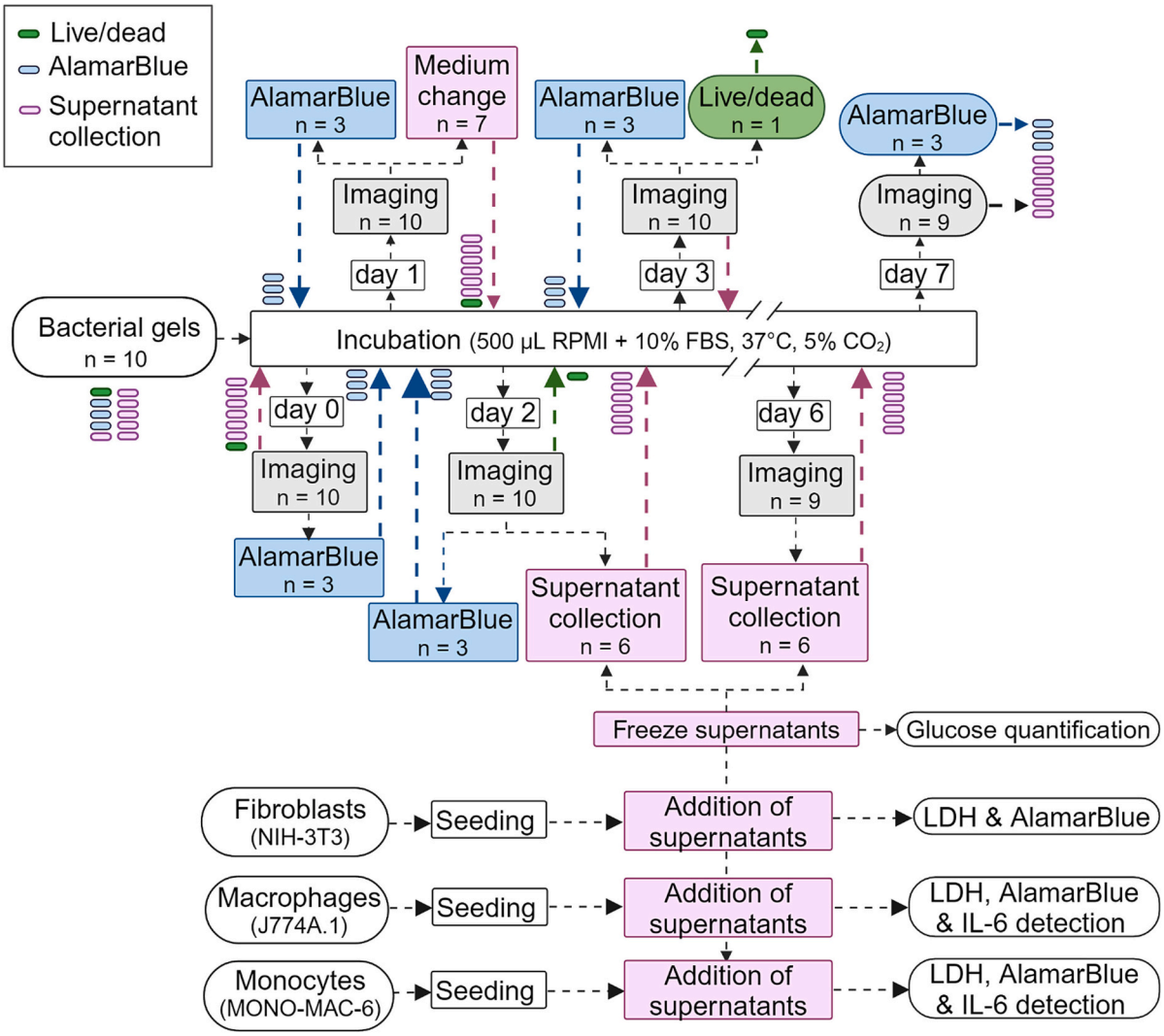


**Fig. 5.** Workflow for in vitro cytocompatibility assessment of LTMs.
The workflow starts with 10 samples and studies LTMs over 7 days. On day 0, brightfield imaging is conducted on all constructs and AlamarBlue assay is carried out on 3 constructs. On day 1, all constructs are imaged, 7 constructs have their medium exchanged and the remaining 3 constructs are used for AlamarBlue assay. On day 2, all constructs are imaged, 3 constructs are used for AlamarBlue assay, and 6 constructs are used to collect bacterial supernatants. The remaining construct is incubated further to be used for Live/Dead assay on day 3, after which it is discarded. On this day also, all constructs are imaged and AlamarBlue assay is conducted with 3 constructs. On day 6, brightfield imaging is conducted on all constructs and bacterial supernatants are collected from 6 constructs. On day 7, brightfield imaging is conducted on all constructs and 3 constructs are used for AlamarBlue assay. Afterwards, all constructs are discarded.

AlamarBlue assay to quantify bacteria growth, (ii) live/dead assay to quantify bacteria fitness, (ii) glucose detection assay to quantify glucose concentration in supernatants, (iii) cytotoxicity assays to assess the cytotoxicity of the supernatants on mammalian cells, and (iv) monocyte activation test to quantify the release of the pro-inflammatory cytokine IL-6. The workflow can be applied to four different conditions run by a single operator on a timescale of 7 d with a 4 h daily dedication.

In this work, the workflow was repeated three times (named I, II, III, where applicable) for samples with four different initial ODs (0, 0.05, 0.5 and 0.8). The results of these experiments are presented in the following paragraphs.

Fig. S4 compares selected microscopy images of samples with initial OD 0.5 at different days corresponding to the 3 repetitions of the workflow. Similar growth status of the colonies was observed, indicating good reproducibility of the sample preparation method.

Fig. 6a shows the quantification of the proliferation of bacteria inside the bilayers by the AlamarBlue assay at days 0 to 7 for samples with different initial ODs. A continuous increase in fluorescence intensity was observed during the first 48 h of incubation. Between days 2 and 7, the fluorescence intensity remained stable for the samples with initial ODs of 0.05 and 0.5 while samples with initial OD 0.8 showed a further increase in fluorescence. The fluorescence values at the different days did not show a dependence on the initial OD. Considering that the colonies are discrete and start from a single bacterium dispersed in the hydrogel, this would mean that colonies in samples with lower OD are larger than in samples with higher initial cell density. This is also observed in the brightfield image: colonies in samples with OD 0.05 are the largest in size and the smallest in number.

Fig. S5 shows the quantification of the proliferation of bacteria inside the bilayers for each of the three runs, with similar results for all OD cases, confirming the robustness of the assay.

We expected the growth rate of the bacteria in the hydrogel to correlate with the consumption of nutrients in the supernatant. We therefore quantified the glucose concentration in the supernatants on days 1 and 5. Glucose is the preferred carbon source for *ClearColi* in aerobic conditions. On day 1, no significant differences in glucose concentration were observed among the samples with or without cells. After 5 days, samples loaded with bacteria showed lower glucose

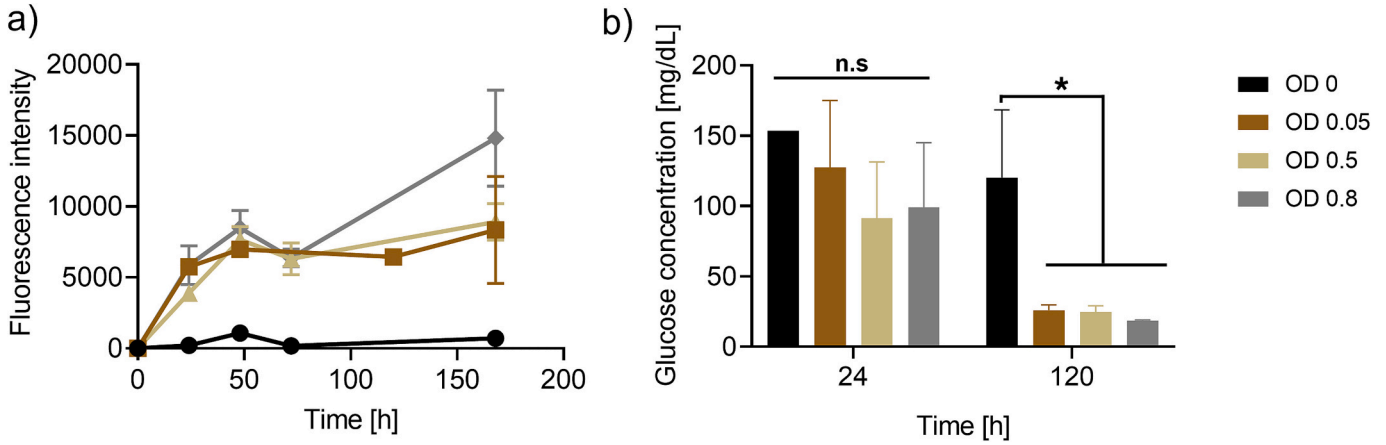


**Fig. 6.** Quantification of bacterial growth and glucose consumption over time.
(a) Fluorescence intensity (arbitrary units) measured from samples after AlamarBlue assay was carried out with different initial bacteria ODs and incubation in RPMI 1640 supplemented with 10 % FBS for 7 d following the workflow (Fig. 4). (b) Concentration of glucose in the supernatants derived from the bilayer thin films with different initial bacteria ODs between 24 h and 5 d of incubation in RPMI 1640 supplemented with 10 % FBS. Empty hydrogels were used as controls. The results represent the mean ± SD of 3 biological replicates.

concentration than controls without bacteria (Fig. 6b), indicating that the living organisms consumed their energy source (Fig. 6b) and in agreement with the slowed down growth of the organisms inside the hydrogel. However, nutrient concentration alone does not seem to be the only factor controlling colony size, since the samples with initial OD 0.8 continued growing from day 5 to day 7.

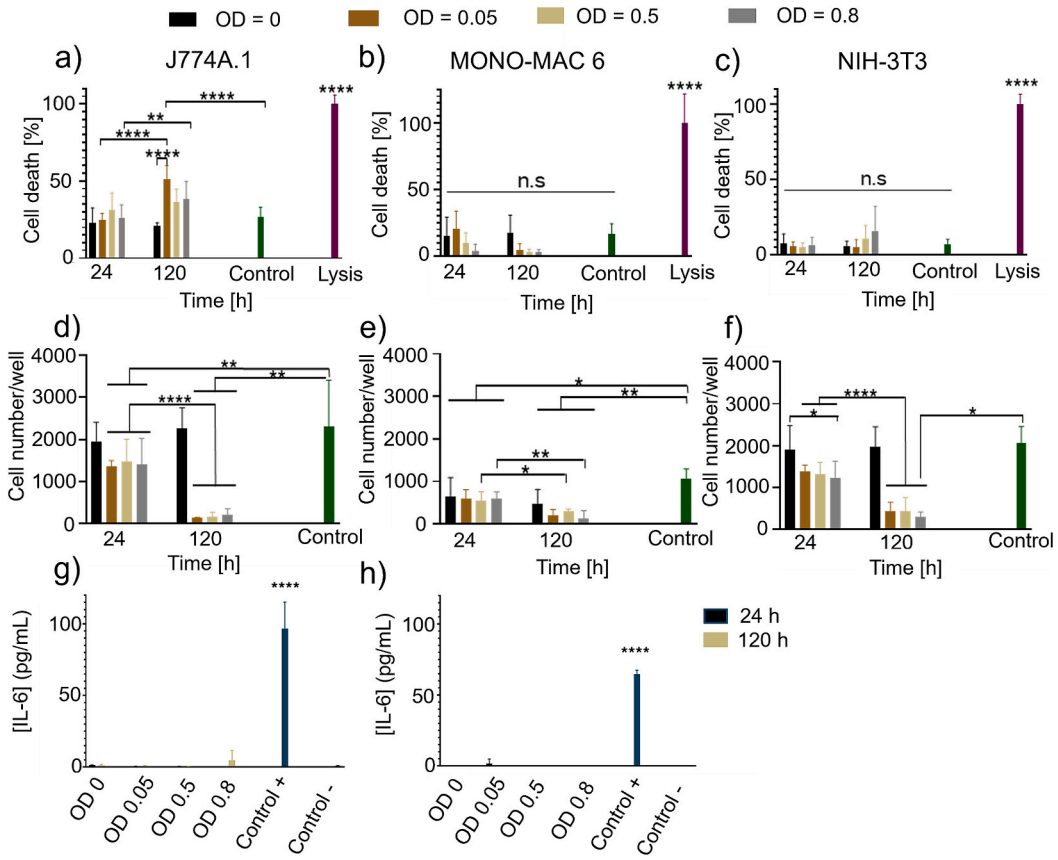


**Fig. 7.** Quantification of cytotoxicity and inflammatory potential of the bilayer thin films.
(a) J774A.1, (b) MONO-MAC-6 and (c) NIH-3 T3 cells with 1- and 5-days supernatants from the bilayer thin films. The controls represent cells treated with the respective cell culture media and the lysis cells treated with Triton-X100. (d–f) AlamarBlue-based number of metabolically active cells after treatment of (d) J774A.1, (e) MONO-MAC-6 and (f) NIH-3 T3 cells with 1- and 5-days supernatants from the bilayer thin films. The controls are representative of cells treated with the respective cell culture media. The cytotoxicity results represent the mean ± SD of 6 biological replicates. (g) Concentration of IL-6 determined after treatment of J774A.1 cells with 1- and 5-days supernatants from bilayer thin films, 15 ng/mL LPS (control +) and cell culture medium (control -). (h) Concentration of IL-6 determined after treatment of MONO-MAC-6 cells with 1- and 5-days supernatants from the bilayer thin films, 15 ng/mL LPS (control +) and cell culture medium (control -) for 24 h. The two latter results represent the mean ± SD of 3 biological replicates.

After investigating the behavior of the bacteria inside the bilayer thin films, we moved to study host response to the LTM secretome by treating three cell lines with the supernatants of the bilayer thin films collected at different timepoints. We selected 24 h supernatant as early time point, when the bacteria are still in the exponential, proliferative phase. As late timepoint, we selected the 120 h supernatant, when proliferation of bacteria has stopped or drastically slowed down (Fig. 7b–h). The selected cell lines were fibroblasts, monocytes and macrophages. Fibroblasts are present in every tissue, being critical players in the foreign body response. Cytotoxicity assays following international standards also suggest the use of fibroblasts for quantification [28]. Monocytes were selected as early players in the foreign body reaction and the main cell type indicative of pyrogenicity potential, i.e., the probability that a compound will provoke fever to the host [29]. Pyrogenicity is an important signal of infection in the body, which is a safety concern for LTMs. Finally, macrophages were also selected as they typically reside in many tissues and are also involved in the late response to foreign body reactions [29].

The cytotoxicity of the supernatants from 1 and 5 days was tested on fibroblasts, monocytes and macrophages (Fig. 7a–f). The integrity of the cell membrane or cell death 24 h after addition of the supernatants was quantified via the lactate dehydrogenase (LDH) assay (Fig. 7a, b, c) The number of metabolically active cells after incubation with the supernatant for 24 h was obtained by AlamarBlue assay (Fig. 7d, e, f). When macrophages were supplied with either 1- or 5-days supernatants, a percentage of cell death around 25–40 % was measured by the LDH assay. This number was similar to the values for the sample with initial OD 0, indicating that the bacteria secretome did not affect the integrity of the cell membrane (Fig. 7a). However, the number of metabolically active macrophages quantified by the AlamarBlue assay was lower than the controls (Fig. 7d). In monocytes treated with the same supernatants, the LDH assay did not reflect cell death after incubation with the supernatant (Fig. 7b), but the AlamarBlue assay reflected a 50 % drop in the number of viable cells (Fig. 7e). Similar results were observed with fibroblasts (Fig. 7c, f).

The inflammatory potential of the supernatants was also characterized. Pyrogenicity was assessed via the monocyte activation test with supernatants from 1 and 5 d (Fig. 7h), and IL-6 secretion was measured with supernatant from 1 d on macrophages (Fig. 7g). No secretion of IL-6 was observed in monocytes after incubation with the supernatants from days 1 and 5 for 24 h, indicating that they were not activated by the secretome of the bacterial hydrogels. Slight amounts of IL-6 were detected in macrophages treated with the supernatant of samples with OD 0.8.

## 4. Discussion

We used Plu/PluDA bilayer thin films as a model LTM to develop a generic workflow for studying the cytocompatibility of LTMs. Before setting the workflow, we characterized key parameters of the bilayer thin films.

As drug delivery systems, LTMs need to allow diffusion of nutrients, metabolites and oxygen to retain the function of the entrapped bacteria and maintain their therapeutic function long term [3]. The burst release of proteins <25 kDa within the first hours correlates with the swelling kinetics of monolayer Pluronic thin films, which reach swelling equilibrium at 6 h [18]. The complete release of proteins with molecular weight < 25 kDa indicates the potential interest of Plu/PluDA hydrogels for the release of biopharmaceuticals from LTMs [30]. Proteins with higher molecular weight diffused up 5–10 % over 4 d, meaning that possible molecules coming from the bacteria (like endotoxin, lipoproteins, flagellins, DNA or RNA) that can be detected as harmful by the host would diffuse at a slower pace, and biocompatibility tests need to consider this long term effects in their design as they would delay immune reaction by the host.

An important molecule regarding the safety of LTMs is DNA, as the possibility of plasmids getting released and being transferred to commensal bacteria might occur. We observed that 6 % of the 6448 bp plasmid entrapped in the hydrogel was released from the bilayer hydrogel in the first 24 h, and afterwards release was very slow and hardly detectable. This result indicates that the hydrogel is permeable to DNA and, therefore, the risk for horizontal gene transfer out of Plu/PluDA hydrogels cannot be excluded. It is noted that DNA can diffuse differently depending on the conformation it adopts and that differences might arise comparing circular DNA diffusion versus linear DNA diffusion in the gels. The probability of occurrence of horizontal gene transfer in this case not only relies on the diffusion of a plasmid but on the acceptance of that plasmid by competent bacteria. Other approaches to reduce the probability of horizontal gene transfer can be adopted, such as the genetic modification of the bacterial genome instead of incorporating the gene cassette of interest via plasmid [31].

Bacterial growth in suspension is mainly governed by nutrient availability and presents 4 phases (lag, exponential, stationery and death) [32]. The lag phase is an adaptation period without growth [33]. The exponential phase is characterized by bacterial proliferation at a constant rate [34]. Once the bacteria run out of nutrients or waste accumulates, bacteria enter the stationary phase. Lastly, the number of viable cells decreases in the death phase [32]. In confinement (e.g. bacteria trapped in a hydrogel matrix), bacteria present different growth kinetics compared to suspension, and it depends on the bacterial strain, culture conditions and the mechanical properties of the matrix confining the bacteria. In previous studies, we observed that the growth kinetics and growth extent of *E. coli* and *Clearcoli* in Plu/PluDA hydrogels [18,20] and *C. glutamicum* in PVA/PVA-VS [35] depend on the shear modulus of the hydrogel, controlled by the degree of covalent crosslinking through the fraction of PluDA or PVA-VS in the hydrogel. In our case, *Clearcoli* within Pluronic-based hydrogels, a growth phase was observed during the first 3 d of culture, which resembled the exponential growth phase of bacteria in suspension, and a slow growth phase was observed from 3 d up to 7 d, which resembled the stationary phase of bacterial growth in suspension (Figs. 3, 4, 6).

Bacteria were alive after encapsulation via photocrosslinking (Fig. S3). We did not expect high photodamage to the bacteria as the irradiation protocol is 1 min at 365 nm and 6 mW/cm$^2$. In a previous study we had irradiated bacteria in suspension for 3 min (365 nm, 6 mW/cm$^2$) and there was no difference in viability and growth compared to the non-irradiated culture [36]. Bacteria also remained alive in the stationary phase up to at least 7 d as confirmed by live/dead staining up to 7 d (Fig. S3). This corroborates that bacteria growth rate in confinement responds to more factors than nutrient availability. Our experiments showed that the samples with initial OD 0.8 continued growing from day 5 to day 7 (Fig. 6a). We explain this effect by the fact that that the maximum colony size in growing bacteria inside a hydrogel with no nutrient restriction is regulated by the mechanical properties of the hydrogel, since the growing colony needs to deform the hydrogel to accommodate the new daughter cells [22]. While colonies in samples with OD < 0.5 reached their maximum size within 5 days, the smaller colonies in hydrogels with initial OD 0.8 were still able to deform the hydrogel and continued growing until day 7.

The cytotoxicity, pyrogenicity and pro-inflammatory assays with fibroblasts, monocytes and macrophages showed a low percentage of cell death, measured as the number of cells with compromised cell membrane, when the cells were treated with LTM supernatants from days 0 to 7. However, quantification of the number of viable cells by AlamarBlue assay showed a decrease in the number of cells after treatment, which was significantly pronounced in samples treated with the 120 h supernatant. This indicates that cells are slowing their metabolic activity. Several reasons could explain this effect. (i) The reduced amount of glucose available in the supernatants at longer time points, as bacteria have consumed around 80 % of the available glucose (Fig. 6b). Monocytes for instance have been shown to express an inflammatory phenotype in both Type 2 Diabetic patients and healthy subjects under low

glucose conditions in vitro [37]. (ii) A higher toxicity of the media by the possible accumulation of metabolites and waste products by bacteria. (iii) The release of PAMPs from the LTMs which, as high molecular weight molecules, is slow (Figs. 2, S2) and would only be noticeable in the supernatant after several days. We would expect PAMP release to activate monocytes and macrophages.

In the monocyte activation test, which measures the pyrogenicity potential by the release of IL-6 after treatment, no IL-6 was detected in culture after treatment with the supernatants at any conditions (Fig. 7). This indicates that the bilayer thin films did not release pyrogens, i.e., any molecule capable of triggering a fever response in the host, PAMP being one example. It is important to note that the presence of endotoxins in our model LTMs is restricted by using the strain *ClearColi* which does not produce LPS. This might be different with other strains. In addition, other molecules could also act as non-endotoxin pyrogens [38]. The fact that monocytes were not activated in this case indicates that there was not presence of non-endotoxin pyrogens either, at least at the timepoints investigated.

Like monocytes, macrophages can become pro-inflammatory when triggered by PAMPs and respond by secreting cytokines such as tumor necrosis factor-α (TNF-α), interleukin-1β (IL-1β) and interleukin 6 (IL-6) [39]. Our results showed no IL-6 secretion by macrophages after treatment with the LTM supernatants from different time points, indicating that the inflammatory phenotype was not triggered at this time scales. These results are in accordance with those from Yamanandra et al., which showed that the encapsulation of *ClearColi* in Pluronic–F127 based hydrogels reduces their immunogenic and cytotoxic potentials on human peripheral blood mononuclear cells (PBMCs) [19]. They also co-cultured ClearColi in suspension in direct contact with PBMCs via transwell and observed low cytotoxicity and low secretion of inflammatory cytokines such as IL-6.

## 5. Conclusions

We developed a workflow to investigate several parameters related to the quality and cytocompatibility of LTMs in vitro in parallel and over 7 days. The workflow contains two parts, one devoted to the investigation of bacterial growth, viability and leakage within the bilayer thin films and a second part focused on the study of cytotoxicity and pro-inflammatory reactions of the bilayer thin film supernatants with three different cell lines. This workflow provides a method to quantify the viability and potential safety of LTMs in vitro in a sequential way. Up to 4 different conditions with 10 samples each could be analyzed in parallel over a period of 7 days with a daily dedication of 4 h, thereby saving time and resources such as kits for the various assays. To demonstrate the applicability of the workflow, we investigated *ClearColi*-laden Pluronic bilayer thin films with four different initial amounts of bacteria. We corroborated that the bilayer thin films were not cytotoxic to mammalian cells and did not induce the release of the pro-inflammatory cytokine IL-6.

## CRediT authorship contribution statement

**Joëlle Aurelie Mekontso:** Writing – review & editing, Writing – original draft, Methodology, Investigation, Formal analysis, Data curation. **Usama Farrukh:** Methodology, Investigation. **Sara Trujillo:** Writing – review & editing, Writing – original draft, Supervision, Project administration, Methodology, Funding acquisition, Data curation. **Aránzazu del Campo:** Writing – review & editing, Writing – original draft, Supervision, Project administration, Data curation, Conceptualization.

## Declaration of competing interest

The authors declare the following financial interests/personal relationships which may be considered as potential competing interests:

Sara Trujillo reports financial support was provided by Deutsche Forschungsgemeinschaft. If there are other authors, they declare that they have no known competing financial interests or personal relationships that could have appeared to influence the work reported in this paper.

## Acknowledgements

ST would like to thank the Deutsche Forschungsgemeinschaft for funding through the grant Safe-LM (DFG GZ: TR 2001/1-1) and the Pharmaceutical Research Alliance Saarland for funding this research work. All authors acknowledge the Leibniz ScienceCampus Living Therapeutic Materials for funding, Fluorescence Microscopy Facility at the INM – Leibniz Institute for New Materials for help and advice with microscopy, and Usama Farrukh and Silke Siegrist at INM for providing pluronic-F127 diacrylate. Authors acknowledge BioRender for making it simple to create scientific illustrations of this work.

## Appendix A. Supplementary data

Supplementary data to this article can be found online at https://doi.org/10.1016/j.bioadv.2025.214182.

## Data availability

Data will be made available on request.

## References

[1] A. Rodrigo-Navarro, S. Sankaran, M.J. Dalby, et al., Engineered living biomaterials. *Nat Rev Mater* 6 (2021) 1175–1190.
[2] Tang, TC., An, B., Huang, Y. et al. Materials design by synthetic biology. Nat. Rev. Mater. 6, 332–350 (2021).
[3] Shrikrishnan Sankaran, et al., Optoregulated drug release from an engineered living material: self-replenishing drug depots for long-term, light-regulated delivery, Small 15 (5) (2019) 1804717.
[4] Zhiyong Sun, et al., Genetically engineered bacterial biohybrid microswimmers for sensing applications, Sensors 20 (1) (2019) 180.
[5] Seung-Gyun Woo, et al., A designed whole-cell biosensor for live diagnosis of gut inflammation through nitrate sensing, Biosens. Bioelectron. 168 (2020) 112523.
[6] Jiahua Pu, et al., "virus disinfection from environmental water sources using living engineered biofilm materials." *advanced*, Science 7 (14) (2020) 1903558.
[7] Charlie Gilbert, et al., Living materials with programmable functionalities grown from engineered microbial co-cultures, Nat. Mater. 20 (5) (2021) 691–700.
[8] Ilya Letnik, et al., Living composites of electrospun yeast cells for bioremediation and ethanol production, Biomacromolecules 16 (10) (2015) 3322–3328.
[9] Carlos A. Mora, et al., Programmable living material containing reporter microorganisms permits quantitative detection of oligosaccharides, Biomaterials 61 (2015) 1–9.
[10] Konstantin Schulz-Schönhagen, Nadine Lobsiger, Wendelin J. Stark, Continuous production of a shelf-stable living material as a biosensor platform, Advanced materials technologies 4 (8) (2019) 1900266.
[11] Yensi Flores Bueso, Panos Lehouritis, Mark Tangney, In situ biomolecule production by bacteria; a synthetic biology approach to medicine, J. Control. Release 275 (2018) 217–228.
[12] Gerber, Lukas C., et al. "Incorporation of penicillin-producing fungi into living materials to provide chemically active and antibiotic-releasing surfaces." *Angewandte Chemie (International ed. in English)* 51.45 (**2012**): 11293–11296.
[13] Lin Zhai, et al., Advances of bacterial biomaterials for disease therapy, ACS Synth. Biol. 13 (5) (2024) 1400–1411, https://doi.org/10.1021/acssynbio.4c00022.
[14] Xinyue Liu, et al., 3D printing of living responsive materials and devices, Adv. Mater. 30 (4) (2018) 1704821.
[15] Mark Mimee, et al., An ingestible bacterial-electronic system to monitor gastrointestinal health, Science 360 (6391) (2018) 915–918.
[16] Shrikrishnan Sankaran, Aránzazu Del Campo, "Optoregulated protein release from an engineered living material." *advanced*, Biosystems 3 (2) (2019) 1800312.
[17] Progress Williams, In Biomedical Engineering: Definitions in Biomaterials, Elsevier, Amsterdam, 1987.
[18] Shardul Bhusari, et al., "encapsulation of bacteria in bilayer Pluronic thin film hydrogels: a safe format for engineered living materials." *biomaterials*, Advances 145 (2023) 213240.
[19] Archana K. Yanamandra, et al., "in vitro evaluation of immune responses to bacterial hydrogels for the development of living therapeutic materials." *biomaterials*, Advances 153 (2023) 213554.
[20] Priyanka Dhakane, Varun Sai Tadimarri, Shrikrishnan Sankaran, Light-regulated pro-Angiogenic engineered living materials, Adv. Funct. Mater. 33 (31) (2023) 2212695.

[21] Maayan Lufton, et al., Living bacteria in thermoresponsive gel for treating fungal infections, Adv. Funct. Mater. 28 (40) (2018) 1801581.
[22] Shardul Bhusari, Shrikrishnan Sankaran, Aránzazu Del Campo, "regulating bacterial behavior within hydrogels of tunable viscoelasticity." *advanced*, Science 9 (17) (2022) 2106026.
[23] Trevor G. Johnston, et al., "compartmentalized microbes and co-cultures in hydrogels for on-demand bioproduction and preservation." *nature*, Communications 11 (1) (2020) 563.
[24] Yifei Lu, et al., Engineering bacteria-activated multifunctionalized hydrogel for promoting diabetic wound healing, Adv. Funct. Mater. 31 (48) (2021) 2105749.
[25] Maayan Lufton, et al., Living bacteria in thermoresponsive gel for treating fungal infections, Adv. Funct. Mater. 28 (40) (2018) 1801581.
[26] Zunzhen Ming, et al., "living bacterial hydrogels for accelerated infected wound healing." *advanced*, Science 8 (24) (2021) 2102545.
[27] Di Biase, Manuela, et al. "Photopolymerization of Pluronic F127 diacrylate: a colloid-templated polymerization." Soft Matter 7.10 (2011): 4928–4937.
[28] Xuemei Liu, et al., A comparison of in vitro cytotoxicity assays in medical device regulatory studies, Regul. Toxicol. Pharmacol. 97 (2018) 24–32.
[29] Anderson, James M., Analiz Rodriguez, and David T. Chang. "Foreign body reaction to biomaterials." *Seminars in immunology*. Vol. 20. No. 2. Academic Press, 2008 .
[30] C. Piñero-Lambea, D. Ruano-Gallego, L.Á. Fernández, Engineered bacteria as therapeutic agents, Curr. Opin. Biotechnol. 35 (2015) 94–102.
[31] Vincent M. Isabella, et al., Development of a synthetic live bacterial therapeutic for the human metabolic disease phenylketonuria, Nat. Biotechnol. 36 (9) (2018) 857–864.
[32] Bruslind, Linda. "General microbiology." (**2023**), pp 70–73.
[33] Michael T. Madigan, John M. Martinko, Jack Parker, Brock Biology of Microorganisms vol. 11, Prentice hall, Upper Saddle River, NJ, 1997.
[34] Regina Bailey, Phases of the bacterial growth curve, ThoughtCo, Jun. 4 (2024).
[35] María Puertas-Bartolomé, et al., Self-lubricating, living contact lenses, Adv. Mater. (2023) 2313848.
[36] Krupansh Desai, et al., A screening setup to streamline in vitro engineered living material cultures with the host, Mater. Today Bio 30 (2025) 101437.
[37] Francesco Piarulli, et al., Low glucose concentrations induce a similar inflammatory response in monocytes from type 2 diabetic patients and healthy subjects, Oxid. Med. Cell. Longev. 2017 (1) (2017) 9185272.
[38] A.L.A.N. Baines, Endotoxin testing, Handbook of Microbiological Quality Control (2000) 144–167.
[39] Antonella Viola, et al., The metabolic signature of macrophage responses, Front. Immunol. 10 (2019) 1462.